Computer Communications 194 (2022) 240–249

Contents lists available at ScienceDirect

Computer Communications

journal homepage: www.elsevier.com/locate/comcom

Optimized resource allocation and time partitioning for integrated communication, sensing, and edge computing network ☆

Kaijun Cheng [a], Xuming Fang [a,*], Xianbin Wang [b]

[a] Key Lab of Information Coding and Transmission, Southwest Jiaotong University, Chengdu 610031, China
[b] Department of Electrical and Computer Engineering, University of Western Ontario, London, ONN6A 5B9, Canada

A R T I C L E I N F O

Keywords:
Wireless communication
Edge computing
Sensing
Resource allocation
Time partitioning

A B S T R A C T

The diverse computational tasks generated from advanced applications are becoming more difficult to process by mobile user equipments due to their limited computing capability and battery supply. With the fast development of wireless technology and infrastructure, edge computing is becoming a paradigm to alleviate these problems by offloading the computation tasks to the edge nodes with more computation resources. In addition, the integrated sensing and communication is a promising technology, where the wireless communication and radar sensing share unified hardware platform and radio resources. In this paper, the capabilities of communication, radar sensing and edge computing are integrated together in the proposed base station architecture to support the comprehensive services of data transmission, target sensing, and edge computing. Based on the proposed scheme, a resource allocation and time partitioning problem is investigated to jointly optimize time partitioning, computation task processing mode selection, spectrum resource allocation and target sensing location selection to maximize the weighted sum of task processing and communication performance while guaranteeing the radar sensing performance. Since the problem is non-convex, we decouple the primal problem into three subproblems which are solved separately. Simulation results show that our proposed scheme outperforms the typical relevant schemes and can converge within an acceptable iterations.

1. Introduction

For the future wireless network, in order to achieve better end-to-end performance, it needs not only the help of radar sensing technique to achieve real-time environmental awareness, but also the aid of high speed of transmission to offload sensory data to edge nodes to make efficient processing, decision and control. Specifically, in the scenario of vehicular network, the vehicle-to-everything communication will be used to offload sensory data among neighboring vehicles and road side units (RSUs), and the edge computing will be used to achieve low processing latency and energy consumption, eventually providing safe and efficient autonomous driving and promoting road traffic congestion control [1,2]. Moreover, with the advantages of flexibility deployment, unmanned aerial vehicle can be applied to carry out sensing missions in complicated environment such as the disaster and sparsely populated areas, where sensory data should be offloaded and computed in a low cost but highly-efficient way [3]. Thus, it is of great significance to investigate the integrated functionalities of radar sensing, task computing and data transmission to meet the needs of all walks of life.

1.1. Backgrounds

1.1.1. Edge computing network

With the unprecedented proliferation of diverse applications (e.g., face recognition, virtual reality, augmented reality, etc.), user equipment (UE) cannot effectively handle the computation tasks generated by these applications due to the limited battery lifetime and processing capability, which often results in high processing latency and battery consumption [4]. By leveraging remote computing resources, cloud computing technology can alleviate the above problem to some extent by offloading the tasks of UEs to the remote cloud [5]. Although the cloud can help UEs process computation tasks, it inevitably incurs extra transmission time, consumes backhaul resources and UE transmission power because of the long distance between the UE and cloud, which is not always conducive to the computation task processing. Recently, mobile edge computing (MEC) technology emerges as a promising solution to alleviate the above difficulties. The edge computing network shifts some computation capabilities from the cloud to the edge which is in close proximity to UEs, herein not only reducing task processing

☆ This document is the results of the research project funded by the NSFC, China under Grant 62071393, NSFC High-Speed Rail Joint Foundation, China under Grant U1834210, Sichuan Provincial Applied Basic Research Project, China under Grant 2020YJ0218, and Fundamental Research Funds for the Central Universities, China under Grant 2682021CF019.

* Corresponding author.
E-mail addresses: kaijuncheng@my.swjtu.edu.cn (K. Cheng), xmfang@swjtu.edu.cn (X. Fang), xianbin.wang@uwo.ca (X. Wang).

https://doi.org/10.1016/j.comcom.2022.07.030
Received 14 February 2022; Received in revised form 16 June 2022; Accepted 20 July 2022
Available online 26 July 2022
0140-3664/

latency and transmission energy consumption, but also saving backhaul bandwidths [6]. Meanwhile, with the help of the advanced wireless communication technologies, the edge offloading procedure is accelerated greatly. Therefore, edge computing networks can take both advantages of the short distance with UEs and the full utilization of edge computing resources.

1.1.2. Integrated sensing and communication network

Disregard the dramatic evolution in the last few decades, wireless networks have been mainly used for data transmission, and never been involved in the perception of the surrounding environment. For the future wireless communication network architecture particularly beyond fifth-generation (B5G) and sixth-generation (6G), both academia and industry are advocating utilizing sensing technology to create a mutually shared communication system with the surrounding environment [7]. The arrival of integrated sensing and communication systems will bring future wireless devices new capabilities of active detection and enhancing location-based services, e.g., indoor positioning, gesture recognition and autonomous driving [8,9]. It establishes sensing links with the environment to perceive necessary information, laying a solid foundation for the subsequent data transmission, analysis and process. This novel enabling method makes everything be connected to achieve collaborative awareness.

Towards this end, integrated sensing and communication technology becomes the basis of realizing efficient coexistence of wireless communication and sensing [10]. It provides various advantages over conventional wireless networks with communication functionality only or with coexisting radar and communication that are separately designed. Firstly, wireless communication and sensing resources can be flexibly reused, so that the sensing functionalities can be superimposed on the communication directly as needed to reduce the deployment cost of individual sensing [7]. In this way, the utilization efficiency of both radio resources and the hardware can be greatly improved. Secondly, both massive multiple-input-multiple-output (MIMO) technology and millimeter-wave (mmWave) communication, which are critical to achieve ultra-high transmission in B5G and 6G, are very helpful to achieve accurate radar sensing (also called target sensing interchangeably) [11]. Thirdly, with the advanced wireless communication, radar sensing can achieve higher resolution, which in turn assisting different critical operations in wireless communication, such as beam training and beam tracking in vehicular networks [7]. Therefore, the integrated sensing and communication technology makes the sensing and communication highly coexisted, leading to significant improvement in both performances.

1.2. Related works

1.2.1. Edge computing system

There have been many works related to the edge computing system [12–25]. We classify them into three categories according to the objective function. First, some works aimed to *minimizing the processing latency of tasks* [12–16]. Liu et al. in [12] investigated an MEC system that allows parallel computation task execution and proposed a stochastic computation task scheduling policy. The works in [13,14] both investigated the task offloading problem in vehicular network. The former considered a multi-vehicle service migration problem and proposed an online algorithm to minimize the long-term service latency, where the constraints of quality of experience and the mobility of serving vehicles are taken into account. The latter considered a problem involving the computation load balance of RSUs and proposed a novel model of task scheduling where the state of the RSUs may dynamically switch between sleep and work. Li et al. in [15] proposed a proactive indexed-based scheduling scheme based on the vehicle mobility and computing capability of the edge server to process real-time computing tasks offloaded by autonomous vehicles. Second, literatures like [17–21] were designed to *minimize the energy consumption of the devices*. Hou et al. in [17] proposed a fog computing aided swarm of drones architecture to enhance the capability of drones swarm handling the computation-intensive tasks. Meanwhile, they formulated an energy consumption minimization problem jointly considering the latency, reliability. Chen et al. in [18] optimized offloading decisions and small base station associations jointly to minimize the total energy consumption of all mobile devices. In literature [19], authors incorporated mmWave to boost offloading rate, and optimized the user association, sub-channel allocation and computation offloading decision to minimize the total energy consumption of all users within the required latency. Tan et al. in [20] focused on the joint problem of task offloading and resource allocation in the orthogonal frequency-division multiple access based multi-user collaborative MEC network where task offloading decision, collaboration decision, subcarrier and power allocation, and computing resource allocation are optimized through a two-level alternation method framework. Third, different from the above works minimizing task processing latency or energy consumption of the devices separately, [22–25] put the two indicators into a single utility function to *minimize the cost of latency and energy consumption*, which can adaptively adjust the corresponding weighting factor. Chen et al. in [22] investigated a relay assisted computation offloading problem to support computation offloading as well as the transfer of locally computed results. In order to fully utilize the benefits of fog computing, Luo et al. in [23] proposed an incentive mechanism to stimulate resource sharing among devices by leveraging coalitional game theory and they derived an efficient scheme to obtain the core solution. Lei et al. in [24] utilized deep reinforcement learning method to solve a joint computation offloading and multi-user scheduling problem under stochastic traffic arrival.

1.2.2. Radar sensing integrated communication system

Due to recent advances in wireless communication system and the demands of sensing capability, the radar sensing integrated communication technology becomes a rapidly growing research field. Relying on the MIMO communication, MIMO radar was proposed to improve the deployment flexibility and radar sensing performance [26]. One researching direction is to *investigate the waveforms of MIMO radar* [27,28]. Liu et al. in [27] studied the waveform design problem for colocated MIMO radar, and proposed a waveform design criterion for omnidirectional beampattern to suppress both auto-correlation and cross-correlation sidelobes of angular waveforms. Sun et al. in [28] evaluated the performance of some typical realistic MIMO radar waveforms instead of the ideal orthogonal MIMO waveform. Another researching direction is focused on *optimizing the communication beamformer of MIMO radar* [29,30]. Liu et al. in [29] considered two options where the first one splits the radar and communication antenna separately while the second one shares all the antennas to form a joint waveform to transmit both radar and communication signals. Then, they optimized the beampattern while guaranteeing the performance of the downlink communications. Liu et al. in [30] proposed a joint beamforming approach for MIMO radar and multiuser MIMO communication sharing spectrum and transmit array where a problem was formulated to optimize the performance of MIMO radar transmit beamforming while meeting communication constraints. [1,31,32] focused on *optimizing the upper layer resource allocation of the communication and radar (CommRadar) system*. Zhang et al. in [1] investigated how to balance the volume of shared messages and constrained resources in fog-based vehicular networks. They formulated an optimization problem to maximize the sum satisfaction of cooperative perception, while satisfying the maximum latency and sojourn time constraints of vehicles. Ju et al. in [31] considered a linear frequency modulated pulse radar and optimized CommRadar mode selection, radar steering direction, communication user scheduling, and time allocation between communication and radar detection to achieve adaptive communication and radar detection scheduling. Wang et al. in [32] exploited non-orthogonal multiple access (NOMA) technology where the superimposed NOMA signal is simultaneously exploited for target sensing.

Besides, a beamforming design problem was formulated to maximize the weighted sum of the communication throughput and the effective sensing power.

1.3. Motivations

1.3.1. Integrated communication, sensing, and edge computing network

Based on our analysis, we find that the current researches lack the integration of radar sensing technology in the edge computing related works. The radar sensing function in the edge computing network not only facilitates the target exploration and perception (i.e., feature extract and information excavated), but also helps the base station (BS) collect sensory data for further data analysis and processing. At this point, it is of great importance and worthiness to introduce the radar sensing capability in the existing edge computing network where BS completes all the tasks of data transmission, radar sensing and edge computing. Thus, the communication, sensing and computation are jointly investigated in this integrated network. After introducing radar sensing functionality, one of the most significant challenges lies in how to manage the orchestration of each traffic, e.g., task offloading, uplink (UL) communication, downlink (DL) communication and radar sensing in the current scheduling period (SP).

Therefore, this paper provides an illuminating insight into the integrated communication, sensing, and edge computing network, and intends to make some preliminary discussions on how the different parameters influence the overall system performance in such a symbiotic system.

1.3.2. Resource allocation and time partitioning scheme

Firstly, in this integrated network, the time-division-multiplexing manner is adopted for the scheduling of different kinds of traffic (i.e., task offloading, UL and DL communication, and radar sensing) under the given duration of SP to control the mutual interference. Since one's performance improvement may degrade the other's, the corresponding time partitioning should be optimized in order to achieve maximal weighted utility in terms of computation task processing latency, UL and DL transmission rate. Secondly, how to allocate the constrained spectrum resources to the task offloading links and communication links should be tackled with the purpose of improving offloading and transmission rate. Thirdly, owing to that the computation tasks need to be processed, the task processing mode should be carefully selected to reduce the processing latency. Lastly, how to select the target sensing locations (TSLs) should be optimized in order to guarantee the target sensing performance.

Therefore, in our proposed integrated communication, sensing, and edge computing network, the time partitioning, spectrum resource allocation, computation task processing mode selection and TSL selection are jointly investigated to achieve maximal weighted sum of task processing and communication performance while guaranteeing the performance of radar sensing.

1.4. Our contributions

1. We introduce a kind of integrated communication, sensing, and edge computing network, where the data transmission, target sensing and edge computing services are incorporated and controlled with the shared spectrum in BS.
2. In this integrated network, we propose a time partitioning scheme where the task offloading, UL and DL communication, and target sensing services are conducted to fulfill the task processing, communication and radar sensing requirements. Based on this, we formulate an optimization problem to maximize the weighted sum of task processing and communication performance while guaranteeing the radar sensing performance.

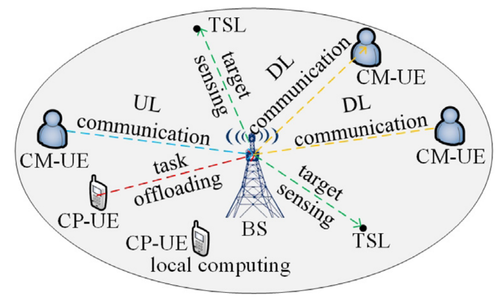

Fig. 1. Model of integrated communication, sensing, and edge computing network.

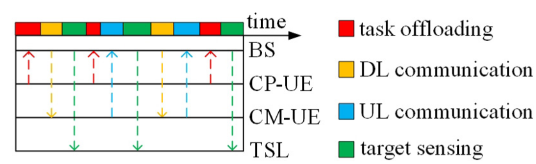

Fig. 2. Illustration of resource allocation and time partitioning scheme in integrated communication, sensing, and edge computing network. (For interpretation of the references to colour in this figure legend, the reader is referred to the web version of this article.)

3. In order to solve this non-convex problem, we decompose the original problem into three subproblems, namely spectrum resource allocation, time partitioning and TSLs selection, and task processing mode selection. We firstly leverage Lagrange duality property and bisection method to solve spectrum resource allocation. Then, we propose a heuristic algorithm to solve time partitioning and TSLs selection. Lastly, we present a coordinate descent (CD) based method to solve task processing mode selection.
4. We prove the convergence of the proposed algorithm and discuss the influence of different parameters on the total utility value. And we also validate the superiority over the comparison schemes.

The remainder of this paper is organized as follows. In Section 2, we give the system model of the integrated network and the illustration of the corresponding resource allocation and time partitioning (RATP) scheme. In Section 3, we give the mathematical models for the task processing, UL and DL communication and radar sensing, and formulate a resource allocation and time partitioning problem. A CD method-based iterative algorithm is designed to solve the above problem in Section 4. Then, we conduct some numerical simulations in Section 5. Lastly, we give the conclusion and present some future work in Section 6.

2. System model and scheme illustration

Fig. 1 shows the model of integrated communication, sensing, and edge computing network, which includes a BS, I communication UEs (CM-UEs), J TSLs and K computation UEs (CP-UEs). BS can conduct series of communication, target sensing and edge computing operations. In order to reduce the hardware complexity, instead of the full-duplex hardware architecture, we assume that BS performs these services by the time sharing and time duplex communication mechanism for all services to avoid mutual interference to each other. In addition, we assume in this paper that at most one CM-UE or CP-UE or TSL could be served at a time. Without loss of generality, the length of SP is denoted by T during which the BS is responsible for four main missions: computation task processing, UL communication, DL communication and target sensing. And the RATP scheme is shown in Fig. 2.

Table 1
System parameters.

Definitions	Notations
Number of CM-UEs, TSLs and CP-UEs	I, J, K
Set of CM-UEs, TSLs and CP-UEs	$\mathcal{I}$, $\mathcal{J}$, $\mathcal{K}$
Length of SP	T
Task size and intensity	l_k, c_k
Task processing mode and TSL selection indicators	ρ_k, b_j
CPU frequency of CP-UE and BS	f_k, f_b
Allocated spectrum for offloading and communication	γ_k^o, γ_i^u, γ_i^d
Transmitting power of CP-UE, CM-UE and BS	p_k^t, p_i^t, p_b^t
Channel power gain between UEs and BS	h_{k_b}, h_{i_b}
Noise power spectral density	N_0
Latency of local computing, offloading and BS computing	$t_{k\_l}^c$, $t_{k\_b}^o$, $t_{k\_b}^c$
Latency of local processing mode and edge processing mode	t_{k_l}, t_{k_b}
Set of tasks computed locally or by BS	K_0, K_1
Offloading rate, UL and DL data rate	r_k^o, r_i^u, r_i^d
Processing latency, UL and DL transmission rate	D_k^{cp}, R_i^{ul}, R_i^{dl}
Allocated time for communication and BS sensing	τ_i^u, τ_i^d, τ_j^s
Coherence processing time	t_j^c
Normalized processing latency, UL and DL transmission rate	$D_k^{cp,n}$, $R_i^{ul,n}$, $R_i^{dl,n}$
Weighting factors for task processing and communication	η^{cp}, η^{ul}, η^{dl}

1. *Computation Task Offloading (the red arrow in Fig. 2)*: Due to the limitation of local computation capabilities of CP-UEs, if they cannot perform the task processing locally, they can offload the tasks to BS for edge computing with the allocated spectrum resources.
2. *UL Communication (the blue arrow in Fig. 2)*: The CM-UEs transmit UL data sequentially to BS with the allocated time and spectrum resources.
3. *DL Communication (the yellow arrow in Fig. 2)*: The BS transmits DL data sequentially to CM-UEs according to the time partitioning and spectrum allocation decisions.
4. *Target Sensing (the green arrow in Fig. 2)*: BS performs target sensing towards TSLs according to the time partitioning and TSL selection results.

3. Mathematical models and problem formulation

In this section, we firstly give the resource allocation models of each traffic, namely computation task processing, UL and DL communication, and target sensing. Then, we formulate the problem as maximizing the weighted sum of task processing and communication performance while guaranteeing the radar sensing performance under the time partitioning, spectrum resources budget, task processing mode selection and radar sensing related constraints. The notations are listed in Table 1 for clarity.

3.1. Resource allocation model

3.1.1. Computation task processing

We characterize an application-generated computation task of CP-UE with two key parameters $\{l_k, c_k\}$, where l_k is the size of computation task (in bits), c_k (in cycles/bit) is the number of computation cycles needed to process one bit of the task. Then, we use a binary variable $\rho_k \in \{0,1\}$ to decide whether the task of CP-UE k is computed locally or offloaded to BS for edge computing. Namely, if the task of CP-UE k is computed locally, $\rho_k = 0$, otherwise $\rho_k = 1$. Thus, if the task of CP-UE k is computed locally, the local computing time is

$$t_{k\_l}^c = \frac{l_k c_k}{f_k}, \forall k \in K_0 \tag{1}$$

where f_k (in CPU cycles/s) is the local CPU frequency of CP-UE k and K_0 indicates the set of tasks computed locally. In the local processing mode, the whole latency t_{k_l} is equal to its local computing time (i.e., $t_{k\_l} = t_{k\_l}^c$).

If the computation task of CP-UE k is offloaded to BS for edge computing, the offloading rate (in bits/s) can be given by

$$r_{k\_b}^o = \gamma_k^o \log_2\left(1 + \frac{p_k^t h_{k\_b}}{\gamma_k^o N_0}\right), \forall k \in K_1 \tag{2}$$

where γ_k^o is the allocated spectrum resources for offloading, p_k^t is the transmitting power of CP-UE k, h_{k_b} is its channel power gain, N_0 is the noise power spectral density and K_1 is the set of tasks offloaded to BS for edge computing.

Then, the offloading latency of CP-UE k can be given by

$$t_{k\_b}^o = \frac{l_k}{r_{k\_b}^o}, \forall k \in K_1 \tag{3}$$

In addition, the time for BS computing the offloaded task from CP-UE k is

$$t_{k\_b}^c = \frac{l_k c_k}{f_b}, \forall k \in K_1 \tag{4}$$

where f_b is the CPU frequency of BS.

Thus, the whole latency if the task of CP-UE k is offloaded to BS for edge computing is the summation of its offloading latency and BS computing latency which is expressed as

$$t_{k\_b} = t_{k\_b}^o + t_{k\_b}^c, \forall k \in K_1 \tag{5}$$

Finally, the processing latency of CP-UE k is

$$D_k^{cp} = (1-\rho_k) t_{k\_l} + \rho_k t_{k\_b}, \forall k \in K \tag{6}$$

Since that the computation result is rather small compared with the task, the time for transmitting computation results back to CP-UEs can be ignored.

3.1.2. UL communication

As for UL communication, the UL data rate of CM-UE i is

$$r_i^u = \gamma_i^u \log_2\left(1 + \frac{p_i^t h_{i\_b}}{\gamma_i^u N_0}\right), \forall i \in I \tag{7}$$

where γ_i^u is the allocated spectrum resources on its UL transmission link, p_i^t is the transmitting power of CM-UE i, h_{i_b} is its channel power gain.

Thus, the UL transmission rate of CM-UE i within SP is

$$R_i^{ul} = \frac{r_i^u \tau_i^u}{T}, \forall i \in I \tag{8}$$

where τ_i^u is the allocated time for CM-UE i UL communication.

3.1.3. DL communication

As for DL communication, the DL data rate of CM-UE i is

$$r_i^d = \gamma_i^d \log_2\left(1 + \frac{p_b^t h_{b\_i}}{\gamma_i^d N_0}\right), \forall i \in I \tag{9}$$

where γ_i^d is the allocated spectrum resources on its DL transmission link, p_b^t is the transmitting power of BS. We assume that the UL and DL links are reciprocal, thus $h_{b\_i} = h_{i\_b}$.

Thus, the DL transmission rate of CM-UE i within SP is

$$R_i^{dl} = \frac{r_i^d \tau_i^d}{T}, \forall i \in I \tag{10}$$

where τ_i^d is the allocated time for CM-UE i DL communication.

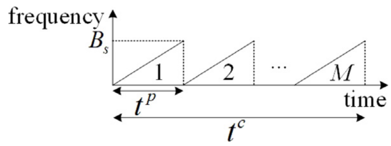

Fig. 3. Model of radar sensing.

3.1.4. Target sensing

Due to its simplicity and low-cost receiver, frequency modulated continuous wave (FMCW) is a commonly used radar waveform [33,34]. For an FMCW radar model shown in Fig. 3, its radar sensing performance (i.e., the false alarm and detection probability performance) can be determined by the signal-to-noise ratio (SNR) of the received echo [35]. We assume the radar waveform consists of M chirp signals, t^p, B_s and S are the duration, sweeping bandwidth and slope of the signal, respectively. The coherent processing time of the radar sensing is denoted as $t^c = Mt^p$, σ_j is the radar cross section (RCS) of the TSL j.

Herein, the echo SNR from TSL j can be written as [35]

$$SNR_j^{echo} = \frac{\sigma_j p_b^t G^t G^r \lambda^2 t_j^c}{(4\pi)^3 (d_{b\_j})^4 N_0 B_s}, \forall j \in J \tag{11}$$

where G^t and G^r are the BS transmitting and receiving antenna gain, λ is its modulated signal wavelength, d_{b_j} is the distance between BS and TSL j.

Given the false alarm and detection probability, we can obtain the echo SNR requirement for TSL j as $SNR_{j\_req}^{echo}$. For the maximum range detection requirement d_{max}, the minimum RCS requirement σ_{min} and echo SNR requirement $SNR_{j\_req}^{echo}$, we can derive

$$t_j^c \geq \frac{SNR_{j\_req}^{echo} (4\pi)^3 (d_{max})^4 N_0 B_s}{\sigma_{min} p_b^t G^t G^r \lambda^2} \tag{12}$$

Thus, the coherent processing time should satisfy

$$t_j^c = \max\left\{ Mt^p, \frac{SNR_{j\_req}^{echo} (4\pi)^3 (d_{max})^4 N_0 B_s}{\sigma_{min} p_b^t G^t G^r \lambda^2} \right\} \tag{13}$$

In order to guarantee the radar sensing performance in terms of range resolution and velocity resolution, as well as false alarm and detection probability, the allocated time for BS sensing the selected TSL j should satisfy

$$\tau_j^s \geq b_j t_j^c, \forall j \in J \tag{14}$$

where τ_j^s is the allocated time for BS performing target sensing towards TSL j, $b_j \in \{0,1\}$ is the selection indicator of TSL j. Specifically, if TSL j is selected for radar sensing, $b_j = 1$, otherwise $b_j = 0$.

3.2. Optimization problem formulation

In order to depict the comprehensive performance, we integrate the processing latency of CP-UEs, UL and DL transmission rate of CM-UEs into a utility function. Since these metrics have different levels of values, we need to conduct normalization operations firstly. Thus, the normalized processing latency of CP-UE k, the normalized UL and DL transmission rate of CM-UE i are

$$D_k^{cp,n} = \begin{cases} 0 & D_k^{cp} \geq D_k^{cp,max} \\ \frac{D_k^{cp,max} - D_k^{cp}}{D_k^{cp,max} - D_k^{cp,min}} & D_k^{cp,min} < D_k^{cp} < D_k^{cp,max} \\ 1 & D_k^{cp} \leq D_k^{cp,min} \end{cases}$$

$$R_i^{ul,n} = \begin{cases} 0 & R_i^{ul} \leq R_i^{ul,th} \\ \frac{R_i^{ul} - R_i^{ul,th}}{R^{ul,max} - R_i^{ul,th}} & R_i^{ul,th} < R_i^{ul} < R^{ul,max} \\ 1 & R_i^{ul} \geq R^{ul,max} \end{cases}$$

$$R_i^{dl,n} = \begin{cases} 0 & R_i^{dl} \leq R_i^{dl,th} \\ \frac{R_i^{dl} - R_i^{dl,th}}{R^{dl,max} - R_i^{dl,th}} & R_i^{dl,th} < R_i^{dl} < R^{dl,max} \\ 1 & R_i^{dl} \geq R^{dl,max} \end{cases}$$

where $\left\{ D_k^{cp,max}, D_k^{cp,min} \right\}$, $\left\{ R^{ul,max}, R_i^{ul,th} \right\}$ and $\left\{ R^{dl,max}, R_i^{dl,th} \right\}$ are the processing latency requirement range for CP-UE k and the UL and DL transmission rate requirement ranges for CM-UE i.

Then, we use a weighted utility function considering the above task processing and communication performances, where this method has been already used in many works such as [25,36].

$$U = \eta^{cp} \sum_{k \in K} D_k^{cp,n} + \eta^{ul} \sum_{i \in I} R_i^{ul,n} + \eta^{dl} \sum_{i \in I} R_i^{dl,n} \tag{15}$$

where $\eta^{cp} \geq 0$, $\eta^{ul} \geq 0$ and $\eta^{dl} \geq 0$ are the corresponding weighting factors. The higher weighting factor means the higher requirement on this service, which also indicates the performance tradeoff among these three services.

In the integrated communication, sensing, and edge computing network, how to partition the time for different kinds of traffic, and allocate the constrained spectrum resources, as well as optimizing the task processing mode selection and TSL selection to achieve the maximum weighted sum of task processing and communication performance while guaranteeing the radar sensing performance needs to be solved. Thus, the resource allocation and time partitioning problem can be formulated as follows

$$\begin{aligned} (P1):\ & \max_{\rho,\gamma,b,\tau} U \\ & \text{s.t. } C1: b_j \in \{0,1\}, \forall j \in J \\ & C2: \sum_{j \in J} b_j \geq b_{req} \\ & C3: \tau_j^s \geq b_j t_j^c, \forall j \in J \\ & C4: \rho_k \in \{0,1\}, \forall k \in K \\ & C5: \gamma_k^o, \gamma_i^u, \gamma_i^d \geq 0, \forall k \in K_1, \forall i \in I \\ & C6: \sum_{k \in K} \rho_k \gamma_k^o + \sum_{i \in I} \left(\gamma_i^u + \gamma_i^d \right) \leq BW \\ & C7: \tau_i^u, \tau_i^d \geq \tau^{min}, \forall i \in I \\ & C8: \sum_{k \in K} \rho_k t_{k\_b}^o + \sum_{j \in J} b_j \tau_j^s + \sum_{i \in I} \left(\tau_i^u + \tau_i^d \right) \leq T \end{aligned} \tag{16}$$

where $\boldsymbol{\rho} \triangleq \{\rho_k\}_{k \in \mathcal{K}}$, $\boldsymbol{\gamma} \triangleq \{\gamma_k^o, \gamma_i^u, \gamma_i^d\}_{k \in \mathcal{K}, i \in \mathcal{I}}$, $\boldsymbol{b} \triangleq \{b_j\}_{j \in \mathcal{J}}$ and $\boldsymbol{\tau} \triangleq \{\tau_i^u, \tau_i^d, \tau_j^s\}_{i \in \mathcal{I}, j \in \mathcal{J}}$. C1 is the constraint for TSL selection. C2 indicates the number of TSLs selected in this radar sensing mission should be greater than the requirement b_{req}. C3 guarantees the radar sensing performance for the selected TSL j. C4 is the constraint for the computation task processing mode selection. C5 and C6 are the spectrum resource limitations and BW is the total available spectrum resources. C7 and C8 are the constraints for time partitioning where τ^{min} is the minimal required time for UL and DL communication.

4. Algorithm design for proposed scheme

Problem $(P1)$ is non-convex due to the combinatorial binary variables and the multiplicative terms in the objective function and constraints C3, C6 and C8. Herein, it is difficult to find its globally optimal solution [32]. In order to solve it, an iterative algorithm is used to obtain a suboptimal solution with low complexity, which is a common methodology to handle the non-convex problem [1,25]. Specifically, we decompose $(P1)$ into three subproblems. Firstly, spectrum resource allocation will be obtained under the given task processing mode selection, time partitioning and TSL selection. Secondly, with the obtained spectrum resource allocation and the given task processing mode selection, the problem of time partitioning and TSL selection will be solved. Thirdly, the problem of task processing mode selection will be solved with the obtained spectrum resource allocation, time partitioning and TSL selection. All the variables will tend to be stable with the iterations going on, and they can be approximated as the solutions of the original problem [37].

4.1. Optimization of spectrum resource allocation

The spectrum resource allocation with the purpose of optimizing the spectrum resources for computation task offloading, UL and DL communication under the given task processing mode selection, time partitioning and TSL selection can be written as

$$\begin{aligned}(P2):\ &\max_{\gamma} \eta^{cp} \sum_{k\in K_1} D_k^{cp,n} + \eta^{ul} \sum_{i\in I} R_i^{ul,n} + \eta^{dl} \sum_{i\in I} R_i^{dl,n} \\ \text{s.t.}\quad & \text{C1: } \gamma_k^o, \gamma_i^u, \gamma_i^d \geq 0, \forall k \in K_1, \forall i \in I \\ & \text{C2: } \sum_{k\in K_1} \gamma_k^o + \sum_{i\in I}\left(\gamma_i^u + \gamma_i^d\right) \leq BW\end{aligned} \tag{17}$$

The first and second order derivatives of $D_k^{cp,n}$ w.r.t offloading rate $r_{k\_b}^o$ are

$$\frac{\partial D_k^{cp,n}}{\partial r_{k\_b}^o} = \frac{l_k}{\left(D_k^{cp,max} - D_k^{cp,min}\right)\left(r_{k\_b}^o\right)^2} \geq 0, \forall k \in K_1 \tag{18}$$

$$\frac{\partial^2 D_k^{cp,n}}{\partial \left(r_{k\_b}^o\right)^2} = \frac{-2l_k}{\left(D_k^{cp,max} - D_k^{cp,min}\right)\left(r_{k\_b}^o\right)^3} \leq 0, \forall k \in K_1 \tag{19}$$

Thus, $D_k^{cp,n}$ is monotonically increasing and concave w.r.t $r_{k\_b}^o$. In addition, the second order derivative of $r_{k\_b}^o$ w.r.t γ_k^o is

$$\frac{\partial^2 r_{k\_b}^o}{\partial \left(\gamma_k^o\right)^2} = \frac{-\left(p_k^t h_{k\_b}\right)^2}{\ln 2\gamma_k^o \left(\gamma_k^o N_0 + p_k^t h_{k\_b}\right)^2} \leq 0, \forall k \in K_1 \tag{20}$$

Obviously, $r_{k\_b}^o$ is concave w.r.t γ_k^o. In addition, $\frac{\partial^2 D_k^{cp,n}}{\partial \gamma_k^o \partial \gamma_{k'}^o} = 0, k \neq k'$. Thus, the Hessian matrix of $\boldsymbol{D^{cp,n}}$ w.r.t $\boldsymbol{\gamma^o}$ is negative definite and is a concave function.

The second order derivative of $R_i^{ul,n}$ w.r.t γ_i^u is

$$\frac{\partial^2 R_i^{ul,n}}{\partial \left(\gamma_i^u\right)^2} = \frac{-\tau_i^u \left(p_i^t h_{i\_b}\right)^2}{T \ln 2 \left(R^{ul,max} - R_i^{ul,th}\right) \gamma_i^u \left(\gamma_i^u N_0 + p_i^t h_{i\_b}\right)^2} \tag{21}$$

It is apparent that $\frac{\partial^2 R_i^{ul,n}}{\partial (\gamma_i^u)^2} \leq 0$, which means $R_i^{ul,n}$ is concave and the Hessian matrix of $\boldsymbol{R^{ul,n}}$ w.r.t $\boldsymbol{\gamma^u}$ is negative definite. Thus, it is also a concave function.

Due to the paper limits, we omit the provement that $\boldsymbol{R^{dl,n}}$ w.r.t $\boldsymbol{\gamma^d}$ is also a concave function which is same with $\boldsymbol{R^{ul,n}}$.

Because of the summation of concave functions is still concave [38], $(P2)$ is a convex optimization problem with linear constraints. We leverage Lagrange duality method to solve this convex optimization problem, based on which the closed-form of the optimal solutions for the spectrum resource allocation can be obtained. The partial Lagrangian function of $(P2)$ is defined as

$$\begin{aligned}\mathcal{L}(\boldsymbol{\gamma}, \upsilon) =& \eta^{cp} \sum_{k\in K_1} D_k^{cp,n} + \eta^{ul} \sum_{i\in I} R_i^{ul,n} + \eta^{dl} \sum_{i\in I} R_i^{dl,n} \\ &+ \upsilon\left(BW - \sum_{k\in K_1} \gamma_k^o - \sum_{i\in I}\left(\gamma_i^u + \gamma_i^d\right)\right)\end{aligned} \tag{22}$$

where υ is a non-negative Lagrangian multiplier to constrain C2 of $(P2)$.

The Lagrangian dual function can be presented as

$$d(\upsilon) = \max_{\gamma} \left\{\mathcal{L}(\boldsymbol{\gamma}, \upsilon) | \gamma_k^o, \gamma_i^u, \gamma_i^d \geq 0, \forall k \in K_1, \forall i \in I\right\} \tag{23}$$

The corresponding dual problem is

$$\min_{\upsilon} \left\{d(\upsilon) | \upsilon \geq 0\right\} \tag{24}$$

Due to that $(P2)$ is a convex problem which satisfies Slater's condition, the dual problem has the same optimal objective value with the primal problem according to the strong duality [38]. Thus, by solving its dual problem in Eq. (24), we can get the solution of $(P2)$.

In the following, we obtain the optimal spectrum resource allocation $\boldsymbol{\gamma^o}$, $\boldsymbol{\gamma^u}$ and $\boldsymbol{\gamma^d}$ for given Lagrangian multiplier υ at first, then the Lagrangian multiplier is obtained via Karush–Kuhn–Tucker (KKT) principle and bisection method.

4.1.1. Update spectrum resource allocation

The first order derivative of $\mathcal{L}(\boldsymbol{\gamma}, \upsilon)$ w.r.t γ_i^u is

$$\frac{\partial \mathcal{L}(\boldsymbol{\gamma}, \upsilon)}{\partial \gamma_i^u} = \frac{\eta^{ul} \tau_i^u \left(\log_2\left(1 + \frac{p_i^t h_{i\_b}}{\gamma_i^u N_0}\right) - \frac{p_i^t h_{i\_b}}{\ln 2 (\gamma_i^u N_0 + p_i^t h_{i\_b})}\right)}{T\left(R^{ul,max} - R_i^{ul,th}\right)} - \upsilon \tag{25}$$

By letting $1 + \frac{p_i^t h_{i\_b}}{\gamma_i^u N_0} = \zeta_i^u$ and setting $\frac{\partial \mathcal{L}(\boldsymbol{\gamma}, \upsilon)}{\partial \gamma_i^u} = 0$ at the optimal point, we have

$$\ln \zeta_i^u + \frac{1}{\zeta_i^u} = 1 + \frac{\left(R^{ul,max} - R_i^{ul,th}\right) \upsilon T \ln 2}{\eta^{ul} \tau_i^u} \tag{26}$$

By taking natural exponential operations at both sides of Eq. (26) and letting $1 + \frac{\left(R^{ul,max} - R_i^{ul,th}\right)\upsilon T \ln 2}{\eta^{ul} \tau_i^u} = \phi_i^u$, we have

$$\zeta_i^u exp\left(\frac{1}{\zeta_i^u}\right) = exp\left(\phi_i^u\right) \tag{27}$$

According to the definition and property of Lambert-W function, we have

$$\frac{1}{\zeta_i^u} = -W\left(-\frac{1}{exp\left(\phi_i^u\right)}\right) \tag{28}$$

Thus, the closed-form solution of γ_i^u is

$$\gamma_i^u = \left[\frac{p_i^t h_{i\_b}}{N_0}\left(\frac{1}{-W\left(-\frac{1}{exp(\phi_i^u)}\right)} - 1\right)^{-1}\right]_0^+ \tag{29}$$

Similarly, the closed-form solutions of γ_i^d and γ_k^o can be derived as

$$\gamma_i^d = \left[\frac{p_b^t h_{b\_i}}{N_0}\left(\frac{1}{-W\left(-\frac{1}{exp(\phi_i^d)}\right)} - 1\right)^{-1}\right]_0^+ \tag{30}$$

$$\gamma_k^o = \left[\frac{p_k^t h_{k\_b}}{N_0}\left(\frac{1}{-W\left(-\frac{1}{exp(\phi_k^o)}\right)} - 1\right)^{-1}\right]_0^+ \tag{31}$$

where $\phi_i^d = 1 + \frac{\left(R^{dl,max} - R_i^{dl,th}\right)\upsilon T \ln 2}{\eta^{dl} \tau_i^d}$, $\phi_k^o = 1 + \frac{\eta^{cp} \upsilon l_k \ln 2}{\left(D_k^{cp,max} - D_k^{cp,min}\right)}$.

4.1.2. Update Lagrangian multiplier

With the achieved spectrum resource allocation $\boldsymbol{\gamma}$, we start to update the Lagrangian multiplier υ. According to the KKT condition, we have

$$\upsilon\left(BW - \sum_{k\in K_1} \gamma_k^o - \sum_{i\in I}\left(\gamma_i^u + \gamma_i^d\right)\right) = 0 \tag{32}$$

Since υ is a non-negative and when $\upsilon \to 0$, $\gamma_k^o \to \infty$, $\gamma_i^u \to \infty$, $\gamma_i^d \to \infty$ according to Eq. (29), Eqs. (30) and (31). Thus, we can conclude that $\upsilon \neq 0$ in Eq. (32). In order to achieve Eq. (32), we can find that

$$\sum_{k\in K_1} \gamma_k^o + \sum_{i\in I}\left(\gamma_i^u + \gamma_i^d\right) = BW \tag{33}$$

Lemma 1. *The left hand of Eq.* (33) *is a monotonically decreasing function w.r.t* υ*, and it has one unique solution* υ^* *that satisfies Eq.* (33)*.*

Proof. The proof is provided in Appendix A. ■

With Lemma 1, the optimal υ^* can be efficiently obtained by bisection method which satisfies Eq. (33), and then the optimal $\boldsymbol{\gamma}^*$ can be derived from Eq. (29), Eqs. (30) and (31). The specific spectrum resource allocation solution for $(P2)$ is shown in Algorithm 1.

Algorithm 1 Spectrum Resource Allocation Solution for ($P2$)

Require: Given time partitioning $\boldsymbol{\tau}$, task processing mode selection $\boldsymbol{\rho}$, accuracy indicator δ, initial upper bound v^{ub} and lower bound v^{lb}

Repeat
  Let $v = \frac{v^{ub}+v^{lb}}{2}$
  Calculate the left hand of Eq. (33) as γ_{total}
  If $\gamma_{total} \geq BW$
    Let $v^{lb} = v$
  Else
    Let $v^{ub} = v$
  EndIf
Until $\left|v^{ub} - v^{lb}\right| \leq \delta$
Obtain optimal spectrum resource allocation by Eq. (29), Eq. (30), Eq. (31)

4.2. Optimization of time partitioning and target sensing location selection

Another subproblem, namely time partitioning and TSL selection is considered to optimize time partitioning for UL and DL communication and target sensing as well as the selection of TSLs with the obtained spectrum resource allocation and the given task processing mode selection, which can be given by

$$
\begin{aligned}
(P3):\ & \max_{\boldsymbol{\tau}} \eta^{cp} \sum_{k\in K} D_k^{cp,n} + \eta^{ul} \sum_{i\in I} R_i^{ul,n} + \eta^{dl} \sum_{i\in I} R_i^{dl,n} \\
& \text{s.t.} \quad \text{C1: } \sum_{j\in J} b_j \geq b_{req} \\
& \text{C2: } \tau_j^s \geq b_j t_j^c, \forall j \in J \\
& \text{C3: } \tau_i^u, \tau_i^d \geq \tau^{min}, \forall i \in I \\
& \text{C4: } \sum_{k\in K_1} t_{k\_b}^o + \sum_{j\in J} b_j \tau_j^s + \sum_{i\in I} \left(\tau_i^u + \tau_i^d\right) \leq T
\end{aligned} \tag{34}
$$

Firstly, we have the following lemma on target sensing after a close observation of ($P3$).

Lemma 2. *The maximal value of utility function achieves when* $\sum_{j\in J} b_j = b_{req}$, $\tau_j^s = b_j t_j^c, \forall j \in J$ *and* $\sum_{k\in K_1} t_{k\_b}^o + \sum_{j\in J} b_j \tau_j^s + \sum_{i\in I} \left(\tau_i^u + \tau_i^d\right) = T$.

Proof. The proof is provided in Appendix B. ■

According to Lemma 2, the solution of TSL selection $\boldsymbol{b}$ and the corresponding time for target sensing $\boldsymbol{\tau}^s$ is shown from step 1 to step 8 of Algorithm 2. Then, ($P3$) can be transferred into ($P4$).

$$
\begin{aligned}
(P4):\ & \max_{\boldsymbol{\tau}^u, \boldsymbol{\tau}^d} \eta^{ul} \sum_{i\in I} R_i^{ul,n} + \eta^{dl} \sum_{i\in I} R_i^{dl,n} \\
& \text{s.t.} \quad \text{C1: } \tau_i^u, \tau_i^d \geq \tau^{min}, \forall i \in I \\
& \text{C2: } \sum_{i\in I} \left(\tau_i^u + \tau_i^d\right) = T - \sum_{k\in K_1} t_{k\_b}^o - \sum_{j\in J} b_j \tau_j^s
\end{aligned} \tag{35}
$$

We regard the subscripts of DL CM-UEs as $i = I+1, I+2, \dots, 2I$. Since the objective function of ($P4$) is monotonically increasing with the time partitioning variables τ_i^u and τ_i^d, we propose a heuristic method to solve it which is shown from step 9 to step 19 of Algorithm 2.

4.3. Optimization of task processing mode selection

With the newly obtained spectrum resource allocation, time partitioning and TSL selection, we leverage CD method which can successively optimize binary variables along the coordinate direction to obtain the local optimum solution [39]. Specifically, starting with an initial $\boldsymbol{g}^0$, we denote $\boldsymbol{g}^r$ as the task processing mode selection decision at the rth iteration. Correspondingly, we denote $U(\boldsymbol{g}^r)$ as the optimal utility value of ($P1$) given $\boldsymbol{g}^r$, which can be obtained by Algorithm 1 and Algorithm 2. And let $\boldsymbol{g}^r(k)$ denotes the task processing mode selection after CP-UE k swapping its current mode, i.e.,

Algorithm 2 Time Partitioning and TSL Selection Solution for ($P3$)

Require: Given task processing mode selection $\boldsymbol{\rho}$ and the optimized spectrum resource allocation $\boldsymbol{\gamma}$

Ensure: Optimized TSL selection $\boldsymbol{b}^*$ and time partitioning $\boldsymbol{\tau}^*$

1: Search for the b_{req} smallest coherent processing time t_j^c and let the corresponding $b_j = 1$
2: For $j \in J$
3:   If $b_j = 1$
4:     Set $\tau_j^s = t_j^c$
5:   Else
6:     Set $\tau_j^s = 0$
7:   EndIf
8: EndFor
9: Let $\tau' = T - \sum_{k\in K_1} t_{k\_b}^o - \sum_{j\in J} b_j \tau_j^s - (2I-1)\tau^{min}$
10: For $q \in 2I$
11:   Let $\tau_q = \tau^{min}$
12: EndFor
13: For $q \in 2I$
14:   Compute $U(q)$ by substituting $\tau_q = \tau'$ into the objective function of ($P4$)
15:   Let $\tau_q = \tau^{min}$
16:   $q = q + 1$
17: EndFor
18: Find the maximal $U(q)$ and obtain the corresponding subscript q'
19: Let $\tau_{q'} = \tau'$

$$
\boldsymbol{g}^r(k) = \left[g_1^r, g_2^r, \dots, g_k^r \oplus 1, \dots, g_K^r\right], \forall k \in K \tag{36}
$$

where $\oplus$ denotes the modulo-2 summation operation.

The task processing mode selection in the rth iteration $\boldsymbol{g}^r$ is determined by the CP-UE that achieves the highest utility value after swapping its processing mode. In other words, $\boldsymbol{g}^r = \boldsymbol{g}^r((k^r)^*)$, where $(k^r)^*=\text{argmax}_{k=1,\dots,K} U(\boldsymbol{g}^r(k))$.

4.4. The overall algorithm for solving (P1)

Based on the above solutions for subproblems, the pseudo-code of the overall algorithm for solving primal problem ($P1$) is illustrated in **Algorithm 3**. Since the outerloop of Algorithm 3 is CD method, whose convergence can be guaranteed [40]. We can conclude that the objective function value of ($P1$) increases monotonically with the iterations, and its optimal value is bounded according to Eq. (15), thus the convergency of **Algorithm 3** can be guaranteed.

5. Simulation results and analysis

In this section, we will present some numerical results to evaluate our proposed RATP scheme for the integrated communication, sensing, and edge computing network. The main simulation parameters are shown in Table 2. The scenario setting indicates the number of CP-UEs, DL and UL CM-UEs. For example, scenario 4 means the numbers of CP-UEs, DL and UL CM-UEs are setting to be (4,4,4). In order to evaluate our proposed scheme and algorithm, we illustrate its performance from three aspects shown in the follows.

5.1. The convergence performance of Algorithm 3

Fig. 4 shows the convergence of the proposed algorithm for solving resource allocation and time partitioning in integrated communication, sensing, and edge computing network. It can be seen that the proposed algorithm can converge within only several iterations w.r.t the total utility in all scenarios, which proves the feasibility and efficiency of our proposed Algorithm 3. And apparently, the total utility value has a positive correlation with the number of UEs.

Algorithm 3 The Overall Algorithm for Solving ($P1$)

Require: Initial task processing mode selection $\boldsymbol{\rho}(0)$, spectrum resource allocation $\boldsymbol{\gamma}(0)$, time partitioning $\boldsymbol{\tau}(0)$, TSL selection $\boldsymbol{b}(0)$, iteration index $r = 0$, algorithm accuracy indicator ϵ and the maximum number of iterations r^{max}

Ensure: Optimized task processing mode selection $\boldsymbol{\rho}^*$, spectrum resource allocation $\boldsymbol{\gamma}^*$, time partitioning $\boldsymbol{\tau}^*$ and TSL selection $\boldsymbol{b}^*$

```
Compute U^0 with the initialized parameters and variables
Repeat
    r = r + 1
    For k ∈ K
    Update g^r(k) using Eq. (36)
        Compute U(g^r(k)) using Algorithm 1 and Algorithm 2
    EndFor
    Let U^r = max_{k=1,...,K} U(g^r(k)) and (k^r)^* = argmax_{k=1,...,K} U(g^r(k))
    Update g^r = g^r((k^r)^*)
Until |U^r − U^{r−1}| ≤ ϵ or r > r^max
```

Table 2
Simulation parameters.

Parameters	Values
Scenario settings	3, 4, 5, 6
Spectrum resource limitation	30 MHz
Distance between BS and UEs	[50, 100] m
Length of SP	2.5 s
Size of computation tasks	[1, 2] Mbits
Complexity of computation tasks	[300, 400] cycles/bit
CPU frequency of CP-UEs	[1, 2] GHz
CPU frequency of BS	8 GHz
Requirement on UL and DL communication time	0.12 s
Transmitting power of UEs	20 dBm
Transmitting power of BS	30 dBm
Coherent processing time	[0.1, 0.2] s
Requirement on the number of TSLs selection	3
Weighting factors for the three kinds of traffic	1, 1, 1

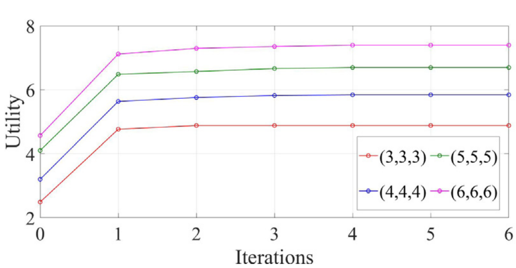

Fig. 4. The convergence behavior of the proposed algorithm.

5.2. The influence of different parameters

Fig. 5 shows the performance of total utility w.r.t the computation task complexity where $c1$, $c2$ and $c3$ are set to be $[200, 300]$ cycles/bit, $[300, 400]$ cycles/bit and $[400, 500]$ cycles/bit. It shows that when the task complexity increases, the total utility value decreases conversely, which indicates that higher task complexity will increase the processing latency of CP-UEs and may result in a situation that CP-UEs choose to offload their tasks to the BS for edge computing, which will share the spectrum resources with CM-UEs, and finally the UL and DL transmission rates decrease.

Fig. 6 presents the influence of local CPU frequency and task size on the total utility under scenario 6, where the values of local CPU are chosen as $[0.5, 1, 1.5, 2, 2.5, 3]$ GHz, and task sizes are $[1, 1.2, 1.4, 1.6, 1.8, 2]$ Mbits, respectively. From the simulation results, we can see that the total utility value increases with the local CPU frequency of CP-UEs. The reason is that the CP-UEs can compute their own computation tasks

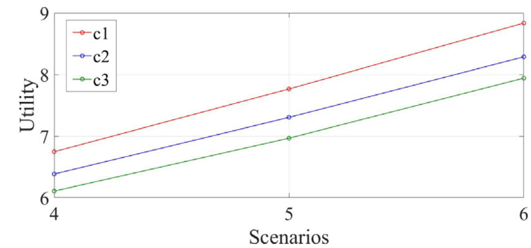

Fig. 5. The total utility versus different levels of computation task complexity.

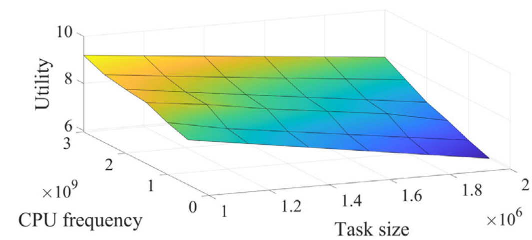

Fig. 6. The total utility versus different task sizes and local CPU frequencies.

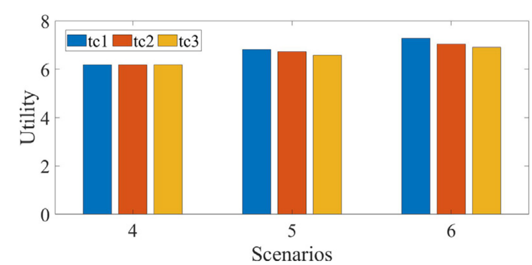

Fig. 7. The total utility versus different target sensing time requirements.

with lower processing latency in terms of higher CPU frequency, which saves spectrum resources for UL and DL communication. Thus, both the processing latency of CP-UEs and transmission rate of UL and DL CM-UEs can be enhanced. As for the influence of computation task size on the total utility, we can see that when the computation task size increases, the total utility value decreases conversely, which indicates that larger task size will increase the processing latency of CP-UEs and may further occupy more spectrum resources on the task offloading procedure. Ultimately, it will deteriorate the performance of UL and DL communication.

The influence of different target sensing time requirements on total utility is shown in Fig. 7, where $tc1$, $tc2$ and $tc3$ are 0 s, 0.2 s and 0.25 s, respectively. It indicates that the performance of radar sensing will increases (i.e., the false alarm and detection probability performance) with larger coherent processing time requirements on the current SP based on the radar detection principle. However, the larger coherent processing time leads to smaller available time of the current SP, which induces less time-domain resources for UL and DL communication. Thus, the total utility value will decrease when the coherent processing time requirements increase. Specifically, $tc1 = 0$ means that there are no TSLs need to be sensed by BS in the current SP, which provides the upper bound performance of our proposed scheme.

In Fig. 8, the performance of total utility w.r.t the different spectrum resource limitations is presented, where $BW1$, $BW2$ and $BW3$ are 20 MHz, 25 MHz and 30 MHz. It shows that with more spectrum resources to be shared among CP-UEs and CM-UEs to support their task offloading, UL and DL communication, the processing latency of task offloading will be reduced, and the transmission rate of UL and DL communication will be improved, thus leading to higher total utility value.

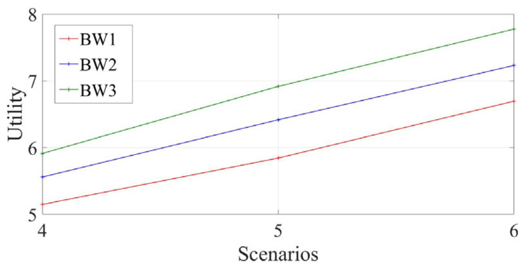

Fig. 8. The total utility versus different spectrum resource limitations.

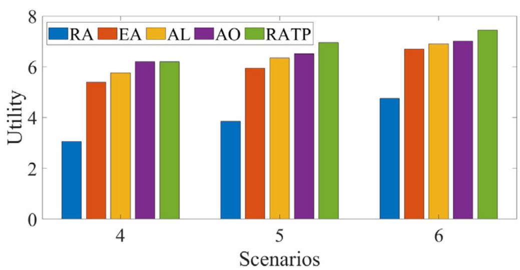

Fig. 9. The total utility comparison with baseline schemes under different scenarios.

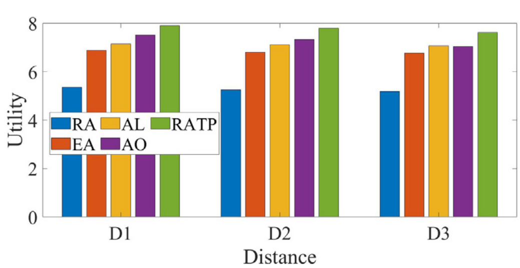

Fig. 10. The total utility comparison with baseline schemes under different distances.

5.3. The performance comparison with baseline schemes

Finally, in order to validate the superiority of our proposed RATP scheme, Figs. 9 and 10 show the total utility comparison with other schemes, namely random allocation scheme (RA), equal allocation scheme (EA), computation task all local processing scheme (AL) and computation task all offloading scheme (AO). In Fig. 9, it shows that the total utility value of the above schemes gradually increases as the number of UEs becomes larger. As we can see, the RA scheme performs worst owing to that the spectrum resources and time partitioning are randomly selected. AL and AO schemes perform better than RA and EA schemes because they optimize the time partitioning and spectrum resource allocation of UL and DL communication which are included in the objective function. Our proposed RATP scheme performs best among them because it iteratively optimizes the task processing mode selection, spectrum resource allocation and time partitioning of UL and DL communication and target sensing. Moreover, Fig. 10 shows the scheme comparison under different distances between BS and UEs where $D1$, $D2$ and $D3$ are $[50, 70]$ m, $[70, 90]$ m and $[90, 110]$ m. And it proves that no matter what distance is, our proposed RATP scheme achieves highest utility value.

6. Conclusion and future work

In this paper, we have investigated the integrated communication, sensing, and edge computing network to meet the requirements of the future wireless system where BS is endowed with the functionalities of UL and DL data transmission, task processing and target sensing. Then, we have proposed a RATP scheme to allocate the spectrum and time resources under this integrated network. Furthermore, we have formulated an optimization problem to maximize the total utility function consisting the normalized task processing latency, UL and DL transmission rate while guaranteeing the performance of radar sensing. In order to solve this non-convex problem, we have decomposed it into three subproblems to optimize spectrum resource allocation, time partitioning, TSL selection and task processing mode selection. Simulation results have confirmed that our proposed algorithm can converge to an optimal point within few iterations. Moreover, we have conducted series of numerical simulations to investigate the influence of parameters of task processing, target sensing and communication on the total utility value. Lastly, we have also validated the superiority of the proposed RATP scheme over other comparison schemes.

For future work, although our proposed RATP scheme is suitable for the specific communication systems, we will further design a more compatible one involving communication, sensing and computation for the general mainstream communication systems, and other radar sensing techniques such as CSI-based sensing will be incorporated. Besides, we will investigate the energy consumption problem in this integrated network since various kinds of traffic consume nonnegligible power, especially in the large-scale network.

CRediT authorship contribution statement

Kaijun Cheng: Conceptualization, Methodology, Software, Investigation, Formal analysis, Validation, Writing – original draft. **Xuming Fang:** Supervision, Resources, Writing – review & editing. **Xianbin Wang:** Supervision, Writing – review & editing.

Declaration of competing interest

The authors declare that they have no known competing financial interests or personal relationships that could have appeared to influence the work reported in this paper.

Appendix A. Proof of Lemma 1

Since $W(x)$ is an increasing function when $x \in (-1/e, 0)$, thus $W\left(-\frac{1}{exp(\phi_i^u)}\right)$ increases when υ increases. Thus, we can conclude that γ_i^u is a monotonically decreasing function w.r.t υ according to Eq. (29). Similarly, γ_i^d and γ_k^o are monotonically decreasing functions w.r.t υ according to Eqs. (30) and (31). Hence, the left hand of Eq. (33) is a monotonically decreasing function w.r.t. υ. In addition, when $\upsilon \to 0$, $W\left(-\frac{1}{exp(\phi_i^u)}\right) \to -1$, thus $\gamma_i^u \to \infty$. Moreover, when $\upsilon \to \infty$, $W\left(-\frac{1}{exp(\phi_i^u)}\right) \to 0$, thus $\gamma_i^u \to 0$. The same conclusions can be applied to γ_i^d and γ_k^o. Hence, it has one unique solution υ^* that satisfies Eq. (33). ■

Appendix B. Proof of Lemma 2

It can be seen from Eqs. (8) and (10) that, with the allocated spectrum resources γ_i^u and γ_i^d, the UL and DL transmission rate of CM-UE i increase monotonically with τ_i^u and τ_i^d. In order to achieve higher value of utility function, the time partitioning for UL and DL communication should be as larger as possible, that is $\sum_{k\in K_1} t_{k\_b}^o + \sum_{j\in J} b_j \tau_j^s + \sum_{i\in I} \left(\tau_i^u + \tau_i^d\right) = T$. And according to C4 of Eq. (34), the allocated time for target sensing should be as smaller as possible while guaranteeing C1 and C2 of Eq. (34). Hence, we can derive $\sum_{j\in J} b_j = b_{req}$ and $\tau_j^s = b_j t_j^c, \forall j \in J$. ■

References

[1] X. Zhang, Z. He, Y. Sun, S. Yuan, M. Peng, Joint sensing, communication, and computation resource allocation for cooperative perception in fog-based vehicular networks, in: 2021 International Conference on Wireless Communications and Signal Processing, WCSP, IEEE, 2021, pp. 1–6.

[2] W. Yue, C. Li, G. Mao, N. Cheng, D. Zhou, Evolution of road traffic congestion control: A survey from perspective of sensing, communication, and computation, China Commun. 18 (12) (2021) 151–177.

[3] T. Li, Z. Cheng, S. Leng, A UAV swarm sensing oriented distributed computing cooperation scheme, in: 2021 IEEE International Conference on Computer and Communication Systems, ICCCS, IEEE, 2021, pp. 168–173.

[4] H. Guo, J. Liu, J. Zhang, Computation offloading for multi-access mobile edge computing in ultra-dense networks, IEEE Commun. Mag. 56 (8) (2018) 14–19.

[5] Z. Chen, J. Hu, G. Min, C. Luo, T. El-Ghazawi, Adaptive and efficient resource allocation in cloud datacenters using actor-critic deep reinforcement learning, IEEE Trans. Parallel Distrib. Syst. (2021) http://dx.doi.org/10.1109/TPDS.2021.3132422.

[6] J. Wang, J. Hu, G. Min, A. Zomaya, N. Georgalas, Fast adaptive task offloading in edge computing based on meta reinforcement learning, IEEE Trans. Parallel Distrib. Syst. 32 (1) (2021) 242–253.

[7] F. Liu, Y. Cui, C. Masouros, J. Xu, T.X. Han, Y.C. Eldar, S. Buzzi, Integrated sensing and communications: Towards dual-functional wireless networks for 6G and beyond, 2021, arXiv preprint, arXiv:2108.07165v1.

[8] B. Sun, Y. Guo, N. Li, L. Peng, D. Fang, TDL: Two-dimensional localization for mobile targets using compressive sensing in wireless sensor networks, Comput. Commun. 78 (2016) 45–55.

[9] C.B. Barneto, S.D. Liyanaarachchi, M. Heino, T. Riihonen, M. Valkama, Full duplex radio/radar technology: The enabler for advanced joint communication and sensing, IEEE Wireless Commun. 28 (1) (2021) 82–88.

[10] Y. Cui, F. Liu, X. Jing, J. Mu, Integrating sensing and communications for ubiquitous IoT: Applications, trends, and challenges, IEEE Netw. 35 (5) (2021) 158–167.

[11] D. Cohen, D. Cohen, Y.C. Eldar, High resolution FDMA mimo radar, IEEE Trans. Aerosp. Electron. Syst. 56 (4) (2020) 2806–2822.

[12] J. Liu, Y. Mao, J. Zhang, K.B. Letaief, Delay-optimal computation task scheduling for mobile-edge computing systems, in: 2016 IEEE International Symposium on Information Theory, ISIT, IEEE, 2016, pp. 1451–1455.

[13] S. Ge, M. Cheng, X. Zhou, Interference aware service migration in vehicular fog computing, IEEE Access 8 (2020) 84272–84281.

[14] Y. Wu, J. Wu, L. Chen, J. Yan, Y. Luo, Efficient task scheduling for servers with dynamic states in vehicular edge computing, Comput. Commun. 150 (2020) 245–253.

[15] M. Li, J. Gao, L. Zhao, X. Shen, Adaptive computing scheduling for edge-assisted autonomous driving, IEEE Trans. Veh. Technol. 70 (6) (2021) 5318–5331.

[16] Z. Liu, Y. Yang, K. Wang, Z. Shao, J. Zhang, POST: Parallel offloading of splittable tasks in heterogeneous fog networks, IEEE Internet Things 7 (4) (2020) 3170–3183.

[17] X. Hou, Z. Ren, J. Wang, S. Zheng, W. Cheng, H. Zhang, Distributed fog computing for latency and reliability guaranteed swarm of drones, IEEE Access 8 (2020) 7117–7130.

[18] H. Chen, D. Zhao, Q. Chen, R. Chai, Joint computation offloading and radio resource allocations in small-cell wireless cellular networks, IEEE Trans. Green Commun. Netw. 4 (3) (2020) 745–758.

[19] Y. Chen, B. Ai, Y. Niu, Z. Zhong, Z. Han, Energy efficient resource allocation and computation offloading in millimeter-wave based fog radio access networks, in: 2020 IEEE International Conference on Communications, ICC, IEEE, 2020, pp. 1–7.

[20] L. Tan, Z. Kuang, L. Zhao, A. Liu, Energy-efficient joint task offloading and resource allocation in OFDMA-based collaborative edge computing, IEEE Trans. Wireless Commun. 21 (3) (2022) 1960–1972.

[21] K. Guo, M. Sheng, J. Tang, T.Q.S. Quek, Z. Qiu, Hierarchical offloading for delay-constrained applications in fog RAN, IEEE Trans. Veh. Technol. 69 (4) (2020) 4257–4270.

[22] X. Chen, Y. Cai, Q. Shi, M. Zhao, B. Champagne, L. Hanzo, Efficient resource allocation for relay-assisted computation offloading in mobile-edge computing, IEEE Internet Things 7 (3) (2020) 2452–2468.

[23] S. Luo, X. Chen, Z. Zhou, X. Chen, W. Wu, Incentive-aware micro computing cluster formation for cooperative fog computing, IEEE Trans. Wireless Commun. 19 (4) (2020) 2643–2657.

[24] L. Lei, H. Xu, X. Xiong, K. Zheng, W. Xiang, X. Wang, Multiuser resource control with deep reinforcement learning in IoT edge computing, IEEE Internet Things 6 (6) (2019) 10119–10133.

[25] Z. Zhao, S. Bu, T. Zhao, Z. Yin, M. Peng, Z. Ding, T.Q.S. Quek, On the design of computation offloading in fog radio access networks, IEEE Trans. Veh. Technol. 68 (7) (2019) 7136–7149.

[26] J. Li, P. Stoica, MIMO Radar Signal Processing, John Wiley & Sons, 2009.

[27] H. Liu, S. Zhou, H. Zang, Y. Cao, Two waveform design criteria for colocated MIMO radar, in: 2014 International Radar Conference, IEEE, 2014, pp. 1–5.

[28] H. Sun, C. Gao, K.C. The, Performance evaluation of practical MIMO radar waveforms, in: 2016 IEEE Radar Conference, RadarConf, IEEE, 2016, pp. 1–6.

[29] F. Liu, C. Masouros, A. Li, H. Sun, L. Hanzo, MU-MIMO communications with MIMO radar: From co-existence to joint transmission, IEEE Trans. Wireless Commun. 17 (4) (2018) 2755–2770.

[30] X. Liu, T. Huang, N. Shlezinger, Y. Liu, J. Zhou, Y.C. Eldar, Joint transmit beamforming for multiuser MIMO communications and MIMO radar, IEEE Trans. Signal Process. 68 (2020) 3929–3944.

[31] H. Ju, Y. Long, X. Fang, Y. Fang, R. He, Adaptive scheduling for joint communication and radar detection: Tradeoff among throughput, delay, and detection performance, IEEE Trans. Veh. Technol. 71 (1) (2022) 670–680.

[32] Z. Wang, Y. Liu, X. Mu, Z. Ding, O.A. Dobre, NOMA empowered integrated sensing and communication, IEEE Commun. Lett. 26 (3) (2022) 677–681.

[33] K.V. Mishra, M.R. Bhavani Shankar, V. Koivunen, B. Ottersten, S.A. Vorobyov, Toward millimeter-wave joint radar communications: A signal processing perspective, IEEE Signal Process. Mag. 36 (5) (2019) 100–114.

[34] S.H. Dokhanchi, B.S. Mysore, K.V. Mishra, B. Ottersten, A mmwave automotive joint radar-communications system, IEEE Trans. Aerosp. Electron. Syst. 55 (3) (2019) 1241–1260.

[35] M.I. Skolnik, Introduction to Radar Systems, McGraw Hill Book Co., New York, 1980.

[36] J. Wang, J. Hu, G. Min, W. Zhan, A. Zomaya, N. Georgalas, Dependent task offloading for edge computing based on deep reinforcement learning, IEEE Trans. Comput. (2021) http://dx.doi.org/10.1109/TC.2021.3131040.

[37] L. Tang, X. Zhang, H. Xiang, Y. Sun, M. Peng, Joint resource allocation and caching placement for network slicing in fog radio access networks, in: 2017 IEEE International Workshop on Signal Processing Advances in Wireless Communications, SPAWC, IEEE, 2017, pp. 1–6.

[38] S. Boyd, L. Vandenberghe, Convex Optimization, Cambridge Univ. Press, Cambridge, U.K., 2004.

[39] S.S. Rao, Engineering Optimization: Theory and Practice, fourth ed., Wiley, Hoboken, NJ, USA, 2009.

[40] S. Bi, Y.J. Zhang, Computation rate maximization for wireless powered mobile-edge computing with binary computation offloading, IEEE Trans. Wireless Commun. 17 (6) (2018) 4177–4190.